

Dipyridyl Amide-Functionalized Polymers Prepared by Ring-Opening-Metathesis Polymerization (ROMP) for the Selective Extraction of Mercury and Palladium

Frank Sinner,[†] Michael R. Buchmeiser,^{*,†} Richard Tessadri,[‡] Mathew Mupa,[†] Klaus Wurst,[§] and Günther K. Bonn[†]

Contribution from the Institutes of Analytical Chemistry and Radiochemistry, of Mineralogy and Petrography, and of General, Inorganic and Theoretical Chemistry, University of Innsbruck, Innrain 52a, A-6020 Innsbruck, Austria

Received October 6, 1997

Abstract: Ring-opening-metathesis polymerization (ROMP) was used for the preparation of a dipyridylcarbamide-functionalized polymer suitable for solid-phase extraction of metal ions from aqueous solutions. Resins were prepared by the copolymerization of the functional monomer *N,N*-di-2-pyridyl-endo-norborn-2-ene-5-carboxamide (**I**) with 1,4,4a,5,8,8a-hexahydro-1,4,5,8-exo-endo-dimethanonaphthalene (**II**), using the well-defined Schrock catalyst Mo(N-2,6-*i*-Pr₂C₆H₃)CHCMe₂Ph(OCMe(CF₃)₂)₂ (**III**). The polymerization proceeds in a living manner, allowing the stoichiometric buildup of polymers. NMR investigations proved the expected backbone structure of the resulting polymers, where the binding site of the monomer remains unaffected in course of the polymerization. The new materials were investigated in terms of their complexation behavior versus a large variety of mono-, di-, tri-, and tetravalent metal ions employing UV-vis spectroscopy as well as AAS and ICP-OES techniques. The polymer-bound dipyridylamide ligand showed excellent selectivity toward Hg²⁺ and Pd²⁺, allowing the selective extraction of both divalent metal ions over a broad range of concentrations from complex mixtures. Due to the stability of the resulting complexes, high loadings of the material with both metals were achieved. To elucidate the chemistry of complexation, X-ray structures of compound (**I**) as well as ESI-MS investigations of the complex of **I** with Pd²⁺ were performed. **I** crystallized in the monoclinic space group *P*2₁/*c*, and forms 1:1 complexes with Pd²⁺ under conditions identical to the SPE experiments.

Introduction

The selective concentration of metal ions from aqueous breakdown solutions or their removal from wastewaters play an important role in many industrial applications as well as in environmental chemistry. Soluble species of mercury, which represents one of the most toxic metals, are either based on inorganic (Hg²⁺) or organometallic (e.g., CH₃Hg⁺) compounds. Despite the usually low concentrations of Hg²⁺ in aqueous wastewaters, its removal therefrom is inevitable.

The platinum group elements (PGEs) consist of Ru, Rh, Pd, Os, Ir, and Pt. Platinum group minerals (PGMs) occur in small amounts in all primary deposits, usually in very fine grain sizes, in association with common nickel, copper, and iron sulfides.¹ The technology of recovering and separating these metals is complicated because of the different PGE-bearing ores, in which the elements occur in varying proportions. The individual deposits require individual treatment, for example the complex Sudbury/Canada deposits, containing a PGE content of roughly 0.5 g/t require several ten of steps until a filtrate containing Pt and Pd as H₂(PtCl₆) and H₂(PdCl₄), respectively, is achieved. The filtrate has to be treated with ammonium hydroxide and

ammonium chloride to obtain (NH₄)₂(PdCl₄). This salt represents the most common starting material for palladium for many industrial processes. It allows the straightforward synthesis of a large variety of organometallic derivatives, where palladium is used both in form of Pd²⁺ salts as well as in form of complexed, zerovalent organometallic compounds. Despite the fact that many technically relevant processes represent catalytic cycles, considerable amounts of the element are lost as a consequence of limited turn-over numbers and are therefore often found in various forms of sludge formed during these degradation processes. The degradation products very often represent complex mixtures of inorganic, organic, and organometallic compounds out of which palladium may be recycled by simply destroying the matrix using breakdown mixtures based onto aqua regia. During the course of this procedure the metal is dissolved and exists in solution in form of H₂PdCl₄. The selective separation of Pd²⁺ (H₂PdCl₄) from other metal ions or from break down solutions represents therefore a straightforward access to its enrichment from ore as well as to the recycling of the metal from industrial processes.

There exist several methods as well as materials for the preconcentration of both mercury und palladium. For analytical purposes, small amounts of palladium may be concentrated and quantified using adsorptive stripping voltammetry² or electrodeposition on tungsten-magnesium alloy.³ Mercury may be

* Corresponding author. Address: Institut für Analytische Chemie und Radiochemie, Universität Innsbruck, Innrain 52 a, A-6020 Innsbruck, Austria. Telephone: +43-(0)512-507-5184. Fax: +43-(0)512-507-2965. E-mail: michael.r.buchmeiser@uibk.ac.at.

[†] Institute of Analytical Chemistry and Radiochemistry.

[‡] Institute of Mineralogy and Petrography.

[§] Institute of General, Inorganic and Theoretical Chemistry.

(1) Tarkian, M.; Bernhardt, H. J. *TMPM - Tschermaks Mineral. Petrogr. Mitt.* 1984, 33, 121–129.

(2) Georgieva, M.; Pihlar, B. *Fresenius J. Anal. Chem.* 1997, 357, 874–880.

(3) Ohta, K.; Ogawa, J.; Mizuno, T. *Fresenius J. Anal. Chem.* 1997, 357, 995–997.

enriched by forming alloys with gold coil. For preparative scale extractions, cation exchangers⁴ or chelating resins⁵ based on iminodiacetic acid (Chelex 100),^{6–12} polyamines (Chelamin),^{13,14} crown ethers,^{15–17} inorganic surfaces (CeO₂),¹⁸ mercaptothiazoles,¹⁹ hydroxyquinolines,²⁰ and dithiocarbamates²¹ are employed. Unfortunately, all these ligands suffer from insufficient selectivity and/or capacity, which significantly reduces or impedes their broad applicability.

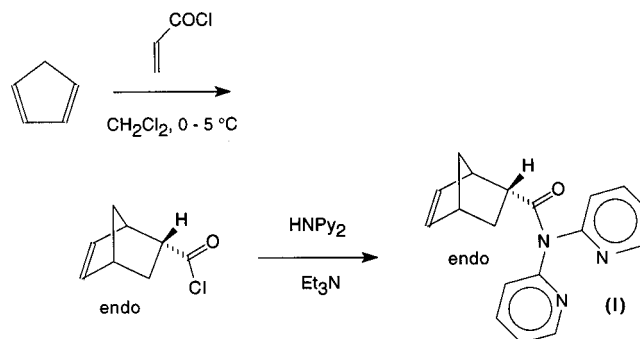
Design of the Resin

Resins for preparative-scale metal ion extraction are usually prepared by surface modification of silica or organic polymers such as poly(styrene divinylbenzene) (PS-DVB). Additionally, several approaches using molecular recognition^{22,23} have been performed. Recently, the preparation of a dithione anchored poly(vinylpyridine)-based chelating resin²⁴ has been reported. This new resin possesses favorable properties in terms of loading capacity, yet no data on the selectivity of the extraction in the presence of all other di- or trivalent metal ions have been presented so far.

A general disadvantage of any derivatization reaction on preformed polymer supports such as silica or PS-DVB lies in the rather poor reaction control. The extent of derivatization is hard to monitor and the nature of the final functional group is often based on assumption rather than on real analysis. Especially with multistep reactions basically any reproducible and predictable synthesis are prevented. The polymerization of functional monomers including the subsequent buildup of beaded particles suitable for separation techniques must therefore be regarded as a challenging, yet promising approach.

To remove mercury or palladium from often complex aqueous solutions, an efficient and selective material is required. The extraction must be efficient both from the economical as well as ecological point of view. Sorbents based on ion exchange usually do not exhibit sufficient selectivity. Polymer-bound crown ethers are available, yet they may not be used for a straightforward synthesis of economically useful materials. A

Scheme 1. Preparation of I



logical consequence was the synthesis of functional polymers containing chelating ligands with a restricted access for many metal ions by a well-defined polymerization method. An additional key requirement was the fact, that the chelating group may not be changed chemically or even stereochemically in course of the polymerization. In this contribution, the preparation and characterization of such a new, selective material, based on a cross-linked dipyridylcarbamide-substituted norbornene, and its use in the selective enrichment of Hg²⁺ and Pd²⁺ are presented.²⁵

Results and Discussion

Polymer Synthesis and Analysis. Recently, Buchmeiser et al.^{26,27} described an entirely different type of carboxylic acid functionalized resins for solid-phase extraction (SPE) with significantly enhanced capacity using ROMP.^{28–30} Following this new concept, dipyridyl amide functionalized resins have been prepared. Synthesis of the starting monomer was achieved by reaction of cyclopentadiene with acrylic acid chloride at 0 °C. A mixture of *exo*- and *endo*-norborn-2-ene-5-carboxylic acid chloride (1:1) was formed. In a second step, this mixture was transformed into the corresponding amide by reaction with *N,N*-di-2-pyridylamine (Scheme 1). Due to steric reasons, only the *endo* isomer reacts with the secondary amine to form *N,N*-di-2-pyridyl-*endo*-norborn-2-ene-5-carbamide. The X-ray structure of this functional monomer is shown in Figure 1.

Crystal Data are given in Table 1, relevant bond distances and angles can be found in Table 2. Atomic coordinates and equivalent isotropic displacement coefficients are shown in Table 3. In the crystal structure, (Figure 1), only the chiral norborn-2-en-5-yl group of the molecule is disordered by overlapping of the enantiomorphic pair with occupancy of 0.5 for each. These two groups, presented in Figure 2, differ slightly in their molecular shapes, and the disordering can be described best by a statistical distribution over the unit cells.

The other part of the molecule is well determined and shows no disorder. This provides important information about relevant bond distances and angles for the interpretation of the selective complexation of mercury and palladium. In the solid state the angle between the nitrogen atom of the carboxylic acid amide

(4) Yang, H.-J.; Huang, K.-S.; Jiang, S.-J.; Wu, C.-C.; Chou, C.-H. *Anal. Chim. Acta* **1993**, *282*, 437.

(5) Fritz, J. S.; Freeze, R. C.; Thornton, M. J.; Gjerde, D. T. *J. Chromatogr. A* **1996**, *739*, 57–61.

(6) Fung, Y. S.; Dao, K. L. *Anal. Chim. Acta* **1995**, *309*, 173–179.

(7) Motellier, S.; Pitsch, H. *J. Chromatogr. A* **1996**, *739*, 119–130.

(8) Pai, S.-C. *Anal. Chim. Acta* **1988**, *211*, 271.

(9) Díaz-Romero, C. *Int. J. Environ. Anal. Chem.* **1996**, *64*, 163–170.

(10) Caroli, S.; Alimonti, A.; Petrucci, F. *Anal. Chim. Acta* **1991**, *248*, 241–249.

(11) Sturgeon, R. E.; Berman, S. S.; Desaulniers, J. A. H.; Mykytiuk, A. P.; McLaren, J. W.; Rusell, D. S. *Anal. Chem.* **1980**, *52*, 1585–1588.

(12) Soldi, T.; Pesavento, M.; Alberti, G. *Anal. Chim. Acta* **1996**, *323*, 27–37.

(13) Groschner, M.; Appriou, P. *Anal. Chim. Acta* **1994**, *297*, 369.

(14) Blain, S.; Appriou, P.; Handel, H. *Anal. Chim. Acta* **1993**, *272*, 91.

(15) Hutchinson, S.; Kearney, G. A.; Horne, E.; Lynch, B.; Glennon, J. D.; McKevey, M. A.; Harris, S. J. *Anal. Chim. Acta* **1994**, *291*, 269–275.

(16) Izatt, R. M.; Bruening, R. L.; Bruening, M. L.; Taret, B.; Krakowiak, K. E.; Bradshaw, J. S.; Christensen, J. J. *Anal. Chem.* **1988**, *60*, 1825.

(17) Billah, M.; Honjo, T. *Fresenius J. Chem.* **1997**, *357*, 61–64.

(18) Vassileva, E.; Varimezova, B.; Hadjiivanov, K. *Anal. Chim. Acta* **1996**, *336*, 141–150.

(19) Filho, N. L. D.; Gushikem, Y.; Polito, W. L. *Anal. Chim. Acta* **1995**, *306*, 167–172.

(20) Landing, W. M.; Haraldsson, C.; Paxéus, N. *Anal. Chem.* **1986**, *58*, 3031.

(21) Rio-Segade, S.; Pérez-Cid, B.; Bendicho, C. *Fresenius J. Anal. Chem.* **1995**, *351*, 798–799.

(22) Matsui, J.; Nicholls, I. A.; Takeuchi, T.; Mosbach, K.; Karube, I. *Anal. Chim. Acta* **1996**, *335*, 71–77.

(23) Izatt, R. M.; Bradshaw, J. S.; Bruening, R. L.; Bruening, M. L. *Am. Lab.* **1994**, *28C*, 28–28M.

(24) Shah, R.; Devi, S. *Anal. Chim. Acta* **1997**, *341*, 217–224.

(25) Buchmeiser, M. R.; Sinner, F.; Tessadri, R.; Bonn, G. K. Austrian Patent Application, A 543/97, patent pending, Apr 1, 1997.

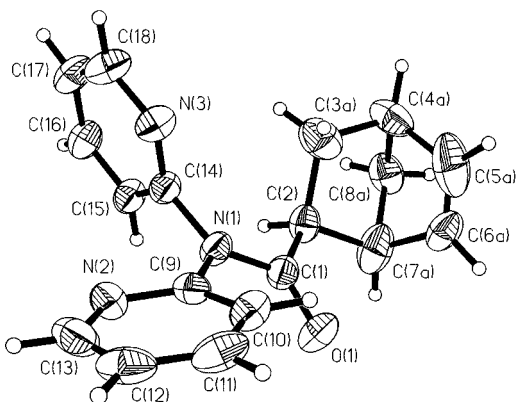
(26) Buchmeiser, M. R.; Atzl, N.; Bonn, G. K., International Patent Application, A 2209/96, PCT AT97/00278, patent pending, Dec 18, 1996.

(27) Buchmeiser, M. R.; Atzl, N.; Bonn, G. K. *J. Am. Chem. Soc.* **1997**, *119*, 9166–9174.

(28) Schrock, R. R. *Ring-Opening Metathesis Polymerization*; Schrock, R. R., Ed.; Hanser: Munich, 1993; p 129.

(29) Schrock, R. R. *Acc. Chem. Res.* **1990**, *23*, 158.

(30) Novak, B. M.; Risse, W.; Grubbs, R. H. *The Development of Well-Defined Catalysts for Ring-Opening Olefin Metathesis Polymerizations (ROMP)*; Polymer Synthesis Oxidation Processes; Springer-Verlag: Berlin, 1992; Vol. 102.

**Figure 1.** X-ray of **I**.**Table 1.** Crystal Data and Structure Refinement for **I**

mol formula	C ₁₈ H ₁₇ N ₃ O
fw	291.35
cryst system	monoclinic
space group	<i>P</i> ₂ / <i>c</i> (no. 14)
unit cell dimens (pm)	<i>a</i> = 1160.8(2); <i>b</i> = 1322.2(3); <i>c</i> = 981.2(2)
β , deg	102.55(2)
vol, nm ³	1.4707(5)
<i>Z</i>	4
<i>T</i> , K	203(2)
radiation	Mo K α (λ = 71.073 pm)
density (calcd), mg/m ³	1.316
abs coeff, mm ⁻¹	0.084
<i>F</i> (000)	616
color, habit	colorless prism
cryst size, mm	0.76 × 0.32 × 0.21
θ range for data collection, deg	3.08–21.0
index range	0 – <i>h</i> – 12, 0 – <i>k</i> – 8, –9 – <i>l</i> – 8
no. of rflns collected	1645
no. of indep rflns	1511
no. of rflns with <i>I</i> > 2 <i>s</i> (<i>I</i>)	1246
refinement method	full-matrix least-squares on <i>F</i> ²
data/restraints/parameters	1451/0/227
goodness of fit on <i>F</i> ²	1.206
final <i>R</i> indices (<i>I</i> > 2 <i>s</i> (<i>I</i>))	<i>R</i> ₁ = 0.0493, <i>wR</i> ² = 0.1111
<i>R</i> indices (all data)	<i>R</i> ₁ = 0.0639, <i>wR</i> ² = 0.1220
largest diff peak and hole, e nm ⁻³	116 and –166

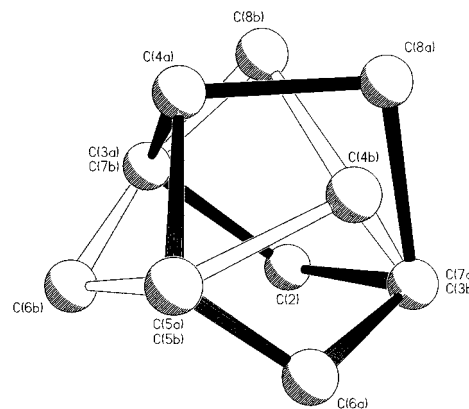
Table 2. Selected Interatomic Distances (pm) and Angles (deg) for **I**

O(1)–C(1)	122.1(4)	N(2)–C(13)	133.2(5)
N(1)–C(1)	139.7(4)	N(2)–C(9)	133.5(4)
C(1)–C(2)	150.5(5)	N(3)–C(14)	133.1(4)
N(1)–C(9)	142.8(4)	N(3)–C(18)	135.2(4)
N(1)–C(14)	143.8(4)		
O(1)–C(1)–C(2)	123.4(3)	C(9)–N(1)–C(14)	116.1(2)
O(1)–C(1)–N(1)	119.5(3)	N(2)–C(9)–N(1)	114.7(3)
N(1)–C(1)–C(2)	117.1(3)	N(3)–C(14)–N(1)	114.3(3)
C(1)–N(1)–C(9)	121.3(3)	C(13)–N(2)–C(9)	117.0(3)
C(1)–N(1)–C(14)	122.6(3)	C(14)–N(3)–C(18)	115.6(3)

and the carbon atoms of the pyridyl groups C(9)–N(1)–C(14) is reduced to 116.1(2)° [120° for sp² hybridization at N(1)]. The planes of the two pyridyl groups are twisted against the plane O(1), N(1), C(1), C(2) and have conformation angles of –139.8(3)° for C(1)–N(1)–C(9)–N(2) and –120.8(3)° for C(1)–N(1)–C(14)–N(3). Therefore the intramolecular distance of the two nitrogen atoms N(2) and N(3) is enlarged to 315.2(4) pm. By twisting the pyridyl groups around the bonds C(9)–N(1) and C(14)–N(1), to get coplanarity with the plane O(1)–N(1)–C(1)–C(2), the distance between N(2) and N(3) decreases to nearly 210 pm. This conflicts with the average N–N distance

Table 3. Atomic Coordinates ($\times 10^4$) and Equivalent Isotropic Displacement Coefficients ($\text{\AA}^2 \times 10^3$) for **I**

	<i>x</i>	<i>y</i>	<i>z</i>	<i>U</i> (eq)	occupancy
O(1)	1504(2)	2481(2)	1225(3)	49(1)	1.0
N(1)	2644(2)	3825(2)	2071(3)	34(1)	1.0
N(2)	4539(2)	3804(2)	1643(3)	42(1)	1.0
N(3)	3027(2)	5519(2)	2643(3)	43(1)	1.0
C(1)	1658(3)	3207(3)	2013(4)	36(1)	1.0
C(2)	833(3)	3485(3)	2942(3)	39(1)	1.0
C(3A)	312(3)	4584(3)	2746(4)	61(1)	0.5
C(4A)	–995(12)	4551(12)	2595(14)	56(4)	0.5
C(5A)	–1337(5)	3988(6)	1120(5)	89(2)	0.5
C(6A)	–1045(7)	3119(7)	1229(9)	48(2)	0.5
C(7A)	–285(4)	2819(3)	2718(4)	62(1)	0.5
C(8A)	–1054(9)	3595(10)	3514(12)	50(3)	0.5
C(3B)	–285(4)	2819(3)	2718(4)	62(1)	0.5
C(4B)	–1279(8)	3430(10)	2438(17)	89(4)	0.5
C(5B)	–1337(5)	3988(6)	1120(5)	89(2)	0.5
C(6B)	–330(11)	4517(10)	1215(11)	99(4)	0.5
C(7B)	312(3)	4584(3)	2746(4)	61(1)	0.5
C(8B)	–819(14)	4289(14)	3340(19)	65(4)	0.5
C(9)	3386(3)	3712(2)	1095(3)	34(1)	0.5
C(10)	2931(3)	3576(2)	–311(3)	40(1)	1.0
C(11)	3706(4)	3517(3)	–1191(4)	50(1)	1.0
C(12)	4898(4)	3626(3)	–647(5)	54(1)	1.0
C(13)	5262(3)	3769(3)	759(5)	51(1)	1.0
C(14)	2997(3)	4582(2)	3131(3)	34(1)	1.0
C(15)	3313(3)	4335(2)	4519(4)	38(1)	1.0
C(16)	3648(3)	5095(3)	5480(4)	45(1)	1.0
C(17)	3671(3)	6076(3)	5012(4)	49(1)	1.0
C(18)	3364(4)	6245(3)	3617(4)	52(1)	1.0

**Figure 2.** Enantiomeric pairs of the 5-substituted norborn-2-ene unit.

for chelating coordination, which is about 280 pm for square planar or octahedral geometry (N–metal–N 90° and metal–N 200 pm). To obtain a distance in this range, the angle C(9)–N(1)–C(14) needs to be enlarged unusually about 20° to 136°. Complexation is therefore believed to occur with both pyridyl groups being not coplanar. As a consequence, the chelating lone pairs of the pyridyl nitrogen atoms are no longer coplanar, too. In this case, the weak complexation with most of the metals results from the fact that only a few metals possess a suitable electron configuration for this type of complexation. According to the HSAB (hard and soft acids and bases) principle, only “soft” metal ions such as Pd²⁺ and Hg²⁺ are capable of rearranging their orbitals in that way.

Data obtained by NMR spectroscopy provide some further insight into the relevant polymer structure of linear poly-**I** which undergoes complexation with the metal ions in the final, cross-linked, beaded material. A non cross-linked, soluble polymer suitable for NMR investigations was prepared by reaction of 10 equiv. of **I** with the initiator **III**, Mo(*N*-2,6-*i*-Pr₂-C₆H₃)-CHCMe₂Ph(OCMe(CF₃)₂)₂ followed by end capping using ferrocene carboxaldehyde. A description of the repetitive unit

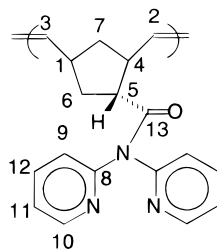


Figure 3. Backbone structure of linear, non-cross-linked poly-I.

of the polymer is given in Figure 3. ^{13}C NMR investigations revealed, that poly-I represents a highly regular polymer. A *cis* assignment for the vinylic protons derived from FT IR data is in accordance with the chemical shifts for C₁ and C₅ (Figure 3) found in polymers with similar structures.³¹

Due to the fact, that I represents a 1:1 mixture of both enantiomers, an equal number of head-to-tail, (HT), tail-to-head (TH), head-to-head (HH), as well as tail-to-tail (TT) assembly modes might be expected in the polymer. In this case, four different signals for the vinylic carbons C₂ and C₃ as well as two sets of signals for the five-membered ring must occur. Surprisingly, the ^{13}C spectrum shows only one set of (broad) signals for C₁ and C₄–C₆, but only one major and another minor set for C₂ and C₃. The ratio of the two sets of the vinylic carbons is about 80:20. This suggests, but yet does not prove, some enantiomer selection by the initiator. On the basis of this set of data, the remaining question relating to the distribution of *m* and *r* dyads cannot be unambiguously defined. Nevertheless, these data allow one to rule out a second way of complexation, where two pyridyl groups from two different adjacent repetitive units form the η^2 -ligand. The roughly 1:1:1:1 random distribution of HH, TH, HT, and TT assemblies allows only 50% of the pyridyl groups to be close enough to form complexes of the general formula L₂PdCl₂ (L = α,α -Py₂-NCO-polymer). In this case, palladium coveries may not be larger than 50% of the theoretical capacity. As a metal uptake of almost 60% may be achieved, this way of complexation seems highly unlikely.

The optimized synthetic route used for the preparation of beaded materials entailed the polymerization of the functional monomer *N,N*-di-2-pyridyl-*endo*-norborn-2-ene-5-carbamide (I) using the well-defined Schrockcatalyst Mo(*N*-2,6-*i*Pr₂C₆H₃)-CHCMe₂Ph(OCMe(CF₃)₂)₂ (III). Subsequent cross-linking using 1,4,4a,5,8,8a-hexahydro-1,4,5,8-*exo,endo*-dimethanonaphthalene (II) resulted in the formation of nonporous particles with an average diameter of 40 μm (Scheme 2). As in the case of previously prepared dicarboxylic acid derivatized resins,²⁷ a major part of the functional groups was again found to be located at the surface of the polymer beads.

Loading experiments revealed an accessibility of the dipyridylcarbamide moieties by palladium of more than 80%. An inverse procedure, starting with the cross-linker II, proved to result in materials with significantly aggravated properties.²⁷ Evidence that the entire polymerization proceeds in a “living”^{32–34} manner is provided by the fact that a plot of equivalents of monomer I added to the initiator III versus the molecular weight of the resulting polymers is linear (Figure 4) and that all samples of capped poly-I prepared in a molecular range of 0–19000 D exhibit a fairly low polydispersity (PDI) (Table 4). The

significantly higher PDIs of 1.6–1.8 compared to a perfectly living system (PDI = 1.00–1.10) may be a consequence of the fact, that I represents a mixture of two enantiomers. The (chiral) propagating species must therefore have different free energies of the transition state ($\Delta\Delta G^\ddagger$) for either of the two enantiomers. As a consequence, the entire system may be considered as a *random AB-block*-polymerization, giving raise to higher dispersity indices. Additionally, a coordination of at least one of the pyridyl groups of I to the molybdenum core must be assumed. Coordination of bases is known to change the electronic situation at the metal center drastically which again often results in higher PDIs.

Due to the fact that the molecular weight of the growing polymer chain increases linearly with the number of monomers added to the system, the actual chain length of poly-I may simply be predetermined by stoichiometry. An additional advantage of the living polymerization is the fact that the initiator derived end of the growing polymer chain remains active after the consumption of I is complete. This allows, upon addition of the cross-linker II, the incorporation of these functional polymers into an entirely cross-linked backbone,^{26,27,35} resulting in a “fur-like” polymer, bearing almost all of its functional groups at the surface. As a consequence, these functionalities are accessible for most analytes within the time scale of a separation. The use of nonliving, prepolymers of I for the formation of particles employing the same cross-linker and stoichiometry, resulted in the formation of materials with entirely different properties. A nonliving system gives rise to polymers with a random distribution of the functional monomer within the particle. As a consequence, a major part of the functional groups is no longer accessible and the material displays significantly impaired properties in terms of particle size, mechanical behavior (swelling), and extraction efficiency.

Following the above-described convergent approach using living systems, two different resins with a dipyridyl amide capacity of 0.6 and 1.0 mequiv/g, respectively, have been prepared in almost quantitative yield. The physical properties of both materials are summarized in Table 5. The rather large particle size (40 μm) allows columns (0.4 \times 6 cm) to be packed without generating a high backpressure. Due to resonance stabilization, the ligand appears to be stable within a pH range of at least 0–12. As a consequence, the resins may be recycled many times. Specific surface areas determined by standard BET experiments were found to be 4–6 m²/g, indicating an entirely nonporous structure. Nevertheless, a certain nonpermanent porosity must be present, leading to an acceptable, yet significant swelling (+34%) of the resins in the conditioned state. This assumption was confirmed by GPC measurements which were performed to determine the specific surface area and the pore volume^{36–38} in the conditioned state. For resin A conditioned in THF, the specific surface area was confirmed to be approximately 4 m²/g. The pore volume was found to be 0.22 mL/g, which provides further evidence for the proposed low porosity.

Selectivity and Extraction Efficiency. An additional advantage of the concept of living polymerizations for resin preparation is based on the fact, that the chelating ligand remains unaffected in terms of its chemical structure and three-dimensional build up during polymerization. This allows, in combination with sufficient knowledge about the backbone

(31) Blackmore, P. M.; Feast, W. J. *Polymer* **1986**, *27*, 1297–1303.

(32) Matyjaszewski, K. *Macromolecules* **1993**, *26*, 1787–1788.

(33) Penczek, S.; Kubisa, P.; Szymanski, R. *Makromol. Chem. Rapid Commun.* **1991**, *12*, 77–80.

(34) Webster, O. W. *Science* **1991**, *251*, 887.

(35) Ambrose, D. L.; Fritz, J. S.; Buchmeiser, M. R.; Atzl, N.; Bonn, G. *J. Chromatogr. A* **1997**, *786*, 259–268.

(36) Knox, J. H.; Scott, H. P. *J. Chromatogr.* **1984**, *316*, 311–332.

(37) Knox, J. H.; Ritchie, H. J. *J. Chromatogr.* **1987**, *387*, 65–84.

(38) Halász, I.; Martin, K. *Angew. Chem.* **1978**, *90*, 954–961.

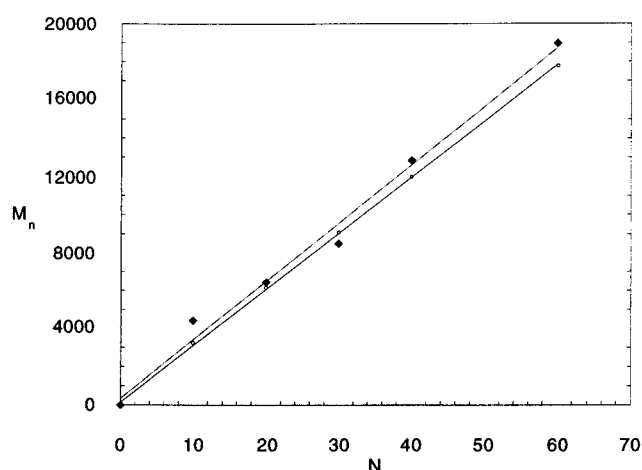
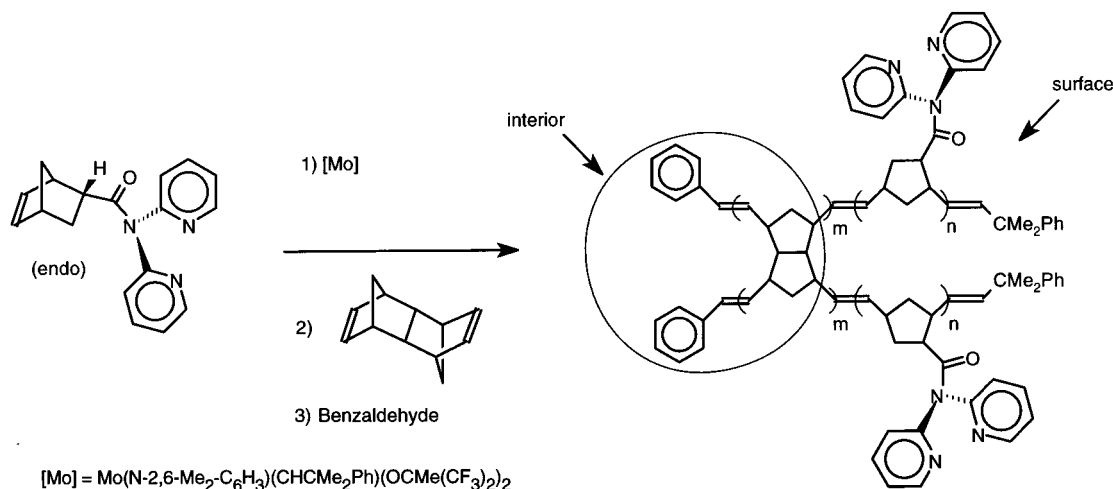
Scheme 2. Preparation of resins A and B using ROMP

Figure 4. Plot of the molecular weight of poly-I versus equivalents of monomer I (from data in Table 4).

Table 4. Summary of Polymerization Results for I^a

equiv of monomer (N)	M _n (found)	M _w (calcd)	PDI (M _w /M _n)
10	3300	3240	1.80
15	4400	4695	1.79
20	6400	6150	1.83
30	8613	9060	1.82
40	12800	11970	1.70
65	18900	19245	1.61

^a Polymerization of N equiv of I using the Schrock initiator III.

Table 5. Physical Properties of Dipyriddylicarbamide Functionalized Resins

resin	bed volume, mL/g	swelling, ^a %	capacity, mequiv/g(Y)	spec surface, m ² /g	yield, %
A	2.2	139	1.0	6 ^b /4 ^c	97.1
B	2.1	135	0.6	4	95.0

^a Conditioned in methanol:water (20:80, v/v). ^b From BET measurements. ^c Calculated from GPC data. Average particle size was 40 ± 10 μm.^{25,26}

structure of the polymer chain, the prediction of the complexation behavior of the final resin based on findings of the complexation chemistry of the monomer.

While many transition metals form stable complexes with imidazole, pyridine, 2,2-dipyridyl, terpyridyl, 1,10-phenanthroline, and 2,2-dipyridylamine,^{39–44} respectively, transformation of the latter compound into an amide changes the electronic situation at all three nitrogens. Additionally, as discussed above, it leads

to the formation of a cavity with significantly restricted access for many cations, resulting in significantly reduced complexing constants for many metal ions. Extraction selectivity was investigated by passing an aqueous solution containing each 5 ppm of Ca²⁺, Sr²⁺, Ba²⁺, Al³⁺, Re³⁺, Fe³⁺, Os⁴⁺, Co²⁺, Rh^{1+/3+}, Ir³⁺, Ni²⁺, Pd²⁺, Pt⁴⁺, Cu²⁺, Ag⁺, Au³⁺, Zn²⁺, Cd²⁺, and Hg²⁺ through an extraction column filled with 100 mg of resin B. Experiments were carried out at a pH of 5.5. During the course of the breakthrough experiments, the effluent was collected in 5 mL portions and checked by ICP–OES. Complete breakthrough for all elements except for Hg²⁺, Pd²⁺, Cu²⁺, and Os⁴⁺ occurred within the first 10 mL. Breakthrough for the latter two elements was observed after 15 mL. These findings are in accordance with the UV–vis investigations performed prior to SPE under noncompetitive conditions. Absorption spectra for the corresponding complexes of the metal ion with I were compared with the spectrum of the free ligand. Normalized spectra, obtained by subtraction of the absorption of both the free metal ion as well as of the free ligand from the spectrum of the corresponding metal–ligand complex, were used throughout. Complexation was unambiguously observed for Hg²⁺, Pd²⁺, Cu²⁺, Os⁴⁺, Rh^{1+/3+}, and Ir³⁺. Figure 5 shows UV–vis spectra of the monomer I and of its complexes with Pd²⁺ and Hg²⁺. The fact, that only these two elements are retained effectively indicate comparably weak complexing constants for all other elements with I. Nevertheless, the stability of certain chloro complexes such as H₂PtCl₆ is believed to play an important role, too.

Detailed investigations on the extraction selectivity and efficiency for both metal ions were performed by variation of pH and concentration. To obtain some insight into kinetics, experiments were carried out using both standard SPE techniques as well as batch experiments.

Selectivity was found to be dependent on the presence of certain inorganic anions. While unbuffered or acetate-buffered

(39) Sandell, E. B.; Onishi, H. *Photometric Determination of Traces of Metals-General Aspects*; Chemical Analysis, 4 ed.; John Wiley & Sons: New York, 1978; Vol. 3.

(40) Perrin, D. D. *Masking and Demasking of Chemical Reactions*; Chemical Analysis; Wiley-Interscience: New York, 1970; Vol. 33.

(41) Livingstone, S. E.; Wheelahan, B. *Aust. J. Chem.* **1964**, *17*, 219–229.

(42) Palmans, R.; MacQueen, D. B.; Pierpont, C. G.; Frank, A. J. *J. Am. Chem. Soc.* **1996**, *118*, 12647–12653.

(43) Hori, H.; Koike, K.; Ishizuka, M.; Westwell, J. R.; Takeuchi, K.; Ibusuki, T.; Ishitani, O. *Chromatographia* **1996**, *43*, 491–495.

(44) Knapp, R.; Schott, A.; Rehahn, M. *Macromolecules* **1996**, *29*, 478–480.

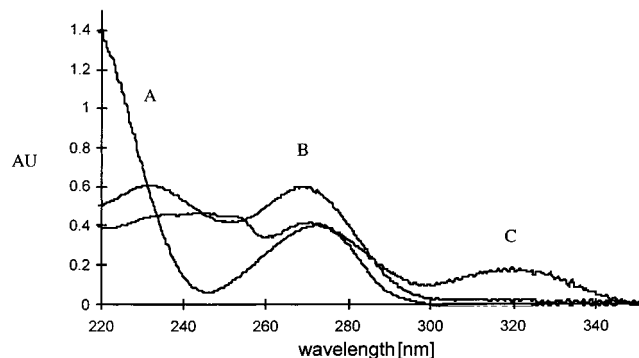


Figure 5. UV-vis absorption spectra in water for complexes of I (spectrum B) with HgCl_2 (spectrum C) and PdCl_2 (spectrum A).

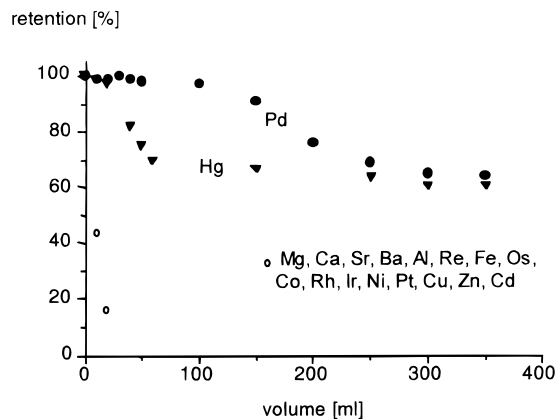


Figure 6. Breakthrough curve of a mixed standard containing each 5 ppm of Mg^{2+} , Ca^{2+} , Sr^{2+} , Ba^{2+} , Re^{3+} , Fe^{3+} , Os^{4+} , Co^{2+} , $\text{Rh}^{+/3+}$, Ir^{3+} , Ni^{2+} , Pd^{2+} , Pt^{4+} , Cu^{2+} , Zn^{2+} , Cd^{2+} , Al^{3+} , Hg^{2+} . PEEK column packed with 100 mg resin A, flow rate 1 mL/min, pH = 5.5. Recorded under competitive conditions.

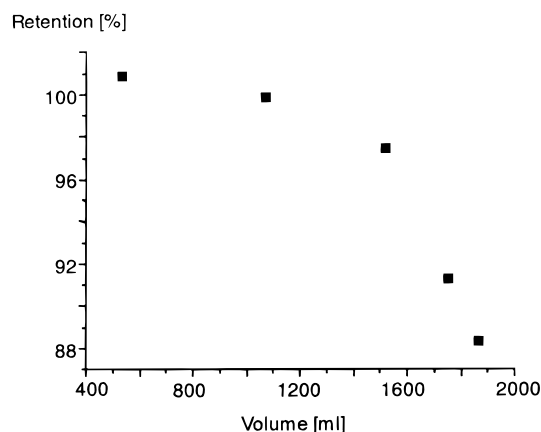


Figure 7. Breakthrough curve of an aqueous 225 ppb HgCl_2 solution (100 mg resin A, flow rate 1 mL/min; pH = 5.5).

systems lead to a decrease in affinity of the corresponding metal ions toward the solid phase in the order $\text{Pd} > \text{Hg} \gg \text{Cu} > \text{Os} > \text{Ir} \sim \text{Rh}$, the presence of phosphate seems to favor the extraction of mercury. Selectivity is changed to the following order: $\text{Hg} > \text{Cu} > \text{Pd} > \text{Os} > \text{Ir} \sim \text{Rh}$. As can be seen from Figure 6, extraction occurs basically only for palladium(II) and mercury(II) in an unbuffered system. The high affinity of the new resins toward these two metal ions is underlined by the fact that these metals may be extracted quantitatively over a broad range of concentrations. Figures 7 and 8 show typical breakthrough curves for the two metal ions at various concentrations.

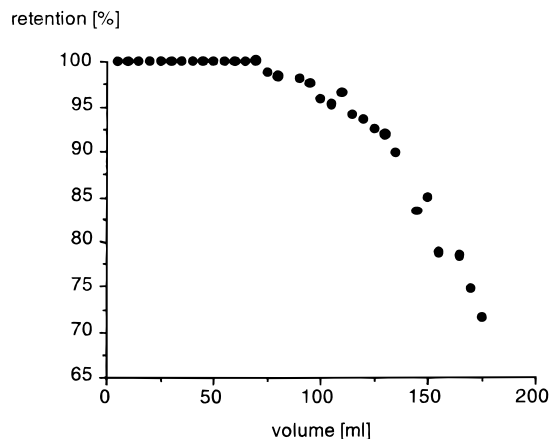


Figure 8. Breakthrough curve of a 20 ppm H_2PdCl_4 standard using 100 mg of resin A (flowrate 1 mL/min; pH = 5.5).

Table 6. Maximum Loadings for Mercury and Palladium

metal ion (concentration)	loading (% of theoretical capacity)
Pd (1%) ^a	57
Pd (1000 ppm) ^a	50
Pd (100 ppm) ^a	42.3
Pd (20 ppm) ^b	14.1
Hg (1%) ^a	52.6
Hg (25 ppm) ^b	2.47
Hg (18 ppm) ^b	2.31
Hg (225 ppb) ^b	1.35

^a Batch experiment, using stirred aqueous solutions. ^b packed columns (0.4 × 6 cm), 100 mg resin A, flow rate.

Another interesting property of this new type of resin for large-scale industrial applications is the fact, that high metal loadings may be achieved. Table 6 gives an overview of the maximum loading prior to breakthrough for different concentrations of the analytes. Additionally, data are given for batch experiments. It can be seen clearly, that high loadings up to 60% and more may be achieved for both metal ions in this type of extraction. This corresponds to an amount of 65 mg of palladium and 120 mg of mercury per gram of resin A, respectively. While both metal ions are extracted with about the same efficiency in a batch experiment, considerable lower loadings of mercury compared to palladium are obtained in a flow through experiment using packed columns. This indicates a higher rate constant for the formation of the palladium complex in comparison with the one for mercury. Once bound to resin, the metals may again be removed therefrom by recomplexation. Thus, elution of a palladium-loaded column with a few milliliters of a solution of thiourea (0.5 M) in 1.5 N HCl or in THF:water (10:90) allows a quantitative recovery (99%) of the metal. The same high recoveries are obtained for a mercury-loaded column using solutions of dimercaptosuccinic acid (DMSA) in THF:methanol (20:80).

Stoichiometry of the Complexes. To discuss capacity-retention relationships, it is important to investigate the actual stoichiometry of the complex formed. While these investigations are hard to perform with stationary phases which have been prepared using a conventional approach, the concept of ROMP allows an in-depth investigation. On the basis of the fact that neither the chemical structure nor the geometry of the ligand are changed significantly in course of the polymerization, the functional monomer itself can be used for these experiments. Aqueous solutions of both HgCl_2 as well as H_2PdCl_4 were treated with an excess of the functional monomer in methanol. A precipitate of the corresponding complex occurred within 2

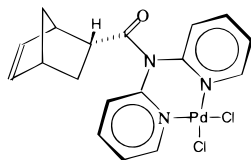


Figure 9. Proposed structure of the monomer palladium complex.

h. Mass spectroscopic investigations using ESI as well as FAB techniques were performed to elucidate the structure of these complexes. Unfortunately, especially the complexes formed with Hg^{2+} exhibited a significantly reduced solubility. This probably results from the fact, that organomercury chlorides tend to form oligomeric structures due to significant μ -bridging of the chlorine atoms. Nevertheless, in the case of palladium, fragments corresponding to $[\text{PdCl}_2(\text{I})\text{K}]^+$ as well as $[\text{Pd}_2\text{Cl}_3(\text{I})_2]^+$ were observed in the ESI-MS mode. These fragments suggest a 1:1 ratio for Pd:(I). This is in accordance with elemental analysis performed on this complex. Further support is provided by the fact, that coveries higher than 50% were found in the case of palladium and mercury. Finally, according to the literature,⁴⁵ compounds such as MCl_2L ($\text{M} = \text{Hg}, \text{Pd}$; $\text{L} = \text{dipyridyl}, 2\text{-picolyamine}$ ⁴⁶) are formed preferably with chloride as a counterion. The complex resulting from the reaction of **I** with Pd^{2+} is therefore believed to have the structure shown in Figure 9, exhibiting presumeably square-planar geometry.

An additional complexation of the 4-coordinate palladium by the carbonyl oxygen may be ruled out by infrared data where a shift from 1680 to 1700 cm^{-1} for the carbonyl group is observed upon complexation with Pd^{2+} .

Conclusions

The new stationary phases bearing the dipyriddy amide ligand prepared by ROMP represent excellent high capacity materials for the enrichment of mercury and palladium out of complex mixtures. The materials are stable within a pH range of 0–12 and may be recycled many times. This and the fact that the extraction proceeds selectively and over a broad range of pH (1–5.5) make these new resins attractive both for analytical as well as preparative scale separations.

Experimental Section

General Details. All synthetic experiments were performed under an argon atmosphere by standard Schlenk techniques unless stated otherwise. Reaction solvents were purified by standard methods. $(\text{NH}_4)_2\text{Mo}_2\text{O}_7$ and ferrocene carboxaldehyde were purchased commercially and used as received. Benzaldehyde and 2,6-diisopropylaniline were distilled prior to use. $\text{Mo}(\text{N}-2,6\text{-iPr}_2\text{C}_6\text{H}_3)(\text{CHCMe}_2\text{Ph})(\text{OCMe}(\text{CF}_3)_2)$ ⁴⁷ and NeophylMgCl⁴⁸ were prepared as described in the literature. Other educts or reagents were prepared according to literature procedures and checked for purity by means of NMR. Reagent-grade pentane, diethyl ether, tetrahydrofuran, toluene, and benzene were distilled from sodium benzophenone ketyl under nitrogen. Reagent-grade dichloromethane was distilled from calcium hydride under argon. All deuterated NMR solvents were dried by appropriate procedures (sodium benzophenone, CaH_2) prior to use. Deionized water was used throughout. Unless stated otherwise, all solvents for analysis

were of p.a. quality and were used without any further purification. Acetonitrile, methanol (both gradient grade), fuming hydrochloric acid 37%, and phosphoric acid 85% were purchased from Merck, Darmstadt, Germany; sodium hydroxide and acetic acid, from Fluka, Buchs, Switzerland; and THF, from Riedel-de Haën (Germany). Aqueous standard solutions (rhenium nitrate, AAS standard solution 1000 ppm in H_2O ; RuCl_3 , AAS standard solution 1000 ppm in H_2O ; IrCl_3 , AAS standard solution 1000 ppm in H_2O ; $\text{H}_2[\text{PdCl}_4]$, AAS standard solution 1000 ppm in H_2O ; $\text{H}_2[\text{PtCl}_4]$, AAS standard solution 1000 ppm in H_2O) were purchased from Johnson Matthey GmbH, Alfa Products. $(\text{NH}_4)_2[\text{OsCl}_6]$, AAS standard solution 1000 ppm in 1 M HCl; $\text{CuSO}_4 \cdot 6\text{H}_2\text{O}$; $\text{ZnSO}_4 \cdot 7\text{H}_2\text{O}$; meso-2,3-dimercaptosuccinic acid (purum (98%)); FeCl_3 , $\text{Zn}(\text{NO}_3)_2 \cdot 6\text{H}_2\text{O}$, $\text{Cu}(\text{NO}_3)_2$; $\text{SnCl}_2 \cdot 2\text{H}_2\text{O}$, $\text{BaCl}_2 \cdot 2\text{H}_2\text{O}$; $\text{Ni}(\text{NO}_3)_2 \cdot 6\text{H}_2\text{O}$; PdCl_2 ; $\text{Ca}(\text{NO}_3)_2 \cdot 4\text{H}_2\text{O}$; and AgNO_3 were purchased from Fluka, Buchs, Switzerland. $[\text{AuCl}_4]$ AAS standard solution 1000 ppm in dilute HCl; $(\text{NH}_4)_3[\text{RhCl}_6]$ AAS standard solution 994 ppm in dilute HCl; $\text{Ca}(\text{NO}_3)_2 \cdot 4\text{H}_2\text{O}$; and AgNO_3 were purchased from Sigma-Aldrich, St. Louis. HgCl_2 subl.; $\text{Cd}(\text{NO}_3)_2 \cdot \text{H}_2\text{O}$; $\text{MgCl}_2 \cdot 6\text{H}_2\text{O}$, >99%; and $\text{Al}(\text{NO}_3)_3 \cdot 9\text{H}_2\text{O}$, $\text{Cd}(\text{NO}_3)_2 \cdot 4\text{H}_2\text{O}$, $\text{Sr}(\text{NO}_3)_2$ were purchased from Merck, Darmstadt, Germany. For all experiments, the SPE materials were first stirred in methanol for 1 h. Slurry packed columns were further conditioned by passing 100 mL of methanol:water (1:1) through the column, followed by 100 mL water (flowrate 3 mL/min). SPE materials used for extraction experiments performed via suspension of the polymer in the corresponding solutions of analytes were stirred for 1 h in methanol:water (1:1) followed by stirring in pure water overnight.

NMR data were obtained in the indicated solvent at 25 °C on a Bruker AM 300 and Varian EM 360L unless stated otherwise and are listed in parts per million downfield from tetramethylsilane for proton and carbon. Coupling constants are listed in Hertz. IR spectra were recorded on a Midac FT IR. Mass spectra were obtained on a CH-7 (MAT). GPC data were determined in CH_2Cl_2 on a Spectroflow 400 using a Water 484 UV-vis detector and a Biorad 1770 Differential Refractometer respectively (flow rate 1 mL/min). Waters Styragel HT 6E columns were used.

UV data were obtained using quartz cuvettes either on a HP 8452A UV detector (range 190–820 nm) in the solvent indicated or on a Perkin-Elmer, Lambda 2 UV-vis-Pecss and are listed in nanometers. Complexation of different elements was studied by recording the UV-vis spectra of (a) pure **I** (0.194 g/L in H_2O), (b) the element (5×10^{-3} g/L in H_2O), and (c) **I** + the corresponding element (0.194 g/L (**I**) + 5×10^{-3} g/L of the element in H_2O). Absorption spectra of **I** with the different elements were obtained by subtraction of the UV-vis spectra of the starting compounds from the resulting spectrum.

Values for the specific pore size and specific surface area^{36–38} of resin A were determined by means of GPC using a Waters 717 Autosampler, a Waters column heater (35 °C), a Waters 510 HPLC pump, a Waters 490E UV detector, a Waters 410 RI detector, and a Millennium work package. Palladium was measured by flame atomic absorption spectroscopy using a Philips PU 9100 X atomic absorption spectrometer (acetylene 0.8 bar, support: fuel ratio 2:1). Mercury was detected by cold vapor AAS, using 10 M NaOH and a 20% SnCl_2 solution. Standard wavelengths for Pd and Hg were 340.5 and 253.7 nm, respectively, using single element hollow cathode lamps (Bachhofer, Germany). A Capex MK II pump from Charles Austem Pump-LTD was used for ventilation. A Philips PU-7000 was used for ICP-OES measurements.

Titration were performed using a 686 Titroprozessor and a 665 Dosimat from Metrohm, Switzerland. To ensure complete deprotonation, resins were stirred overnight in 10% NEt_3 , filtered (G 4), washed with water and dried overnight under vacuum. Finally, the resins were stirred in 10 mL of 0.05 M HCl for 2 h, subsequently filtered, and washed. The combined washings were titrated with 0.05 M NaOH.

Breakthrough curves were recorded using a Waters 501 HPLC pump (Millipore) or a Gilson Miniplus 2 peristaltic pump. Omegachrom PEEK columns (Upchurch scientific, 2×5 cm i.d.) and Knauer steel columns (3.175×6 cm i.d.) were employed. The flowrate was adjusted to 1 mL/min. Unless stated otherwise, the volume of each fraction was 5 mL. With the use of this setup, HgCl_2 solutions (25 ppm, 18 ppm, 225 ppb; pH 5.0) and $\text{H}_2[\text{PdCl}_4]$ solutions (20 ppm; pH 5.5) as well as mixed standards (Ca^{2+} , Sr^{2+} , Ba^{2+} , Re^{3+} , Fe^{3+} , Os^{4+} , Co^{2+} ,

(45) Greenwood, N. N.; Earnshaw, A. *Chemie der Elemente*; VCH: Weinheim, 1988.

(46) Rau, T.; Shoukry, M.; van Eldik, R. *Inorg. Chem.* **1997**, *36*, 1454–1463.

(47) Oskam, J. H.; Fox, H. H.; Yap, K. B.; McConville, D. H.; O'Dell, R.; Lichtenstein, B. J.; Schrock, R. R. *J. Organomet. Chem.* **1993**, *459*, 185.

(48) Schrock, R. R.; Sancho, J.; Pedersen, S. F. *Inorg. Synth.* **1989**, *26*, 44.

Rh⁺³⁺, Ir⁺³⁺, Ni⁺²⁺, Pd⁺²⁺, Pt⁺⁴⁺, Cu⁺²⁺, Ag⁺¹⁺, Au⁺³⁺, Zn⁺²⁺, Cd⁺²⁺, Hg⁺²⁺, and Al⁺³⁺, 5 ppm each, pH 5.5) were passed through a slurry packed column, using the resin quantities indicated in the tables.

Recoveries were determined under noncompetitive conditions by passing a 20 ppm H₂PdCl₄ (pH 5.5) and 20 ppm HgCl₂ (pH 5.3) solution manually through a slurry packed filtration column (Isolute Accessories, 100 mg resin). Pd²⁺ was eluted with 5 mL of 0.5 M thiourea in 1.5 M HCl, respectively. Hg²⁺ was eluted with 10 mL of 0.2 M *meso*-2,3-dimercaptosuccinic acid in THF: methanol (20:80). for the determination of the recoveries for aqueous solutions containing 225 ppb Hg²⁺, 500 mL were passed through a slurry packed PEEK-column (flowrate 1 mL/min, 200 mg resin) and eluted with 5 mL 0.2 M *meso*-2,3-dimercaptosuccinic acid in THF:methanol = (20:80).

Extraction efficiencies for stirred solutions (batch experiments) were determined by quantification of the corresponding element in solution before and after stirring with the resin. Typical procedures were as follows: 100 mg resin were (a) stirred for 4 h in 25 mL of a 20 ppm Hg solution (pH = 5.5), (b) stirred for 16 h in 20 mL of a 1% Hg solution (pH = 5.5), (c) stirred for 4 h in 16 mL of a 90 ppm PdCl₂ solution (pH = 5.5), (d) stirred for 48 h in 100 mL of a 100 ppm PdCl₂ solution, or (e) stirred for 13 h in 20 mL of a 0.1 and 1% PdCl₂ solution, respectively (pH 5.5). Prior to measurement, solutions were passed through a 0.45 μm cellulose-acetate filter (CA-filter) (Satorius, Germany).

endo-Norborn-2-ene-5-carboxylic Acid Chloride. The compound was prepared by reaction of freshly cracked 1,3 cyclopentadiene (54 mL, 0.65 mol.), cooled to 0–5 °C, with acrylic acid chloride (50 mL, 0.62 mol). The reaction mixture was stirred for 30 min and finally distilled under reduced pressure. The *exo* and *endo* isomers were obtained at bp_{exo} = 50 °C/20 mm and bp_{endo} = 70 °C/20 mm. *endo*-Norborn-2-ene-5-carboxylic acid chloride: ¹H NMR (CDCl₃) δ 6.26 (dxd, 1H, J₁ = 3.00, J₂ = 8.8), 5.96 (dxd, 1H, J₁ = 3.00, J₂ = 8.2), 3.43 (m, 1H), 2.98 (bs, 2H), 1.56 (m, 1H), 1.53 (m, 1H), 1.40 (bs, 1H), 1.32 (bs, 1H). *exo*-Norborn-2-ene-5-carboxylic acid chloride: ¹H NMR (CDCl₂) δ 6.26 (dxd, 1H, J₁ = 3.00, J₂ = 9.00), 6.04 (m, 1H), 3.43 (m, 1H), 2.98 (bs, 2H), 1.54 (m, 1H), 1.49 (m, 1H), 1.35 (m, 1H), 1.31 (m, 1H).

N,N-Bipyridyl-endo-norborn-2-ene-5-carbamide. A solution of norborn-2-ene-5-carboxylic acid chloride (10.2 mL, 65.62 mmol) in dry methylene chloride (100 mL) was cooled to –90 °C. A solution of 2,2'-dipyridylamine (11.1 g, 64.8 mmol) in 100 mL dry methylene chloride was added dropwise over a period of 10 min. The reaction mixture was warmed to room temperatures and stirred for 5 h. A total of 20 mL of 15% sodium hydroxide solution was added, and the alkaline solution was extracted with methylene chloride. The combined organic extracts were dried over sodium sulfate and filtered, and the solvent was removed in vacuo. The remaining brown, oily liquid was dried under high vacuum until a light brown residue was obtained. It was dissolved in diethyl ether and filtered through silica gel-60. The ether solution was concentrated and placed in a deep freezer. **I** was isolated in 48% yield (9.1 g). IR (KBr, cm⁻¹): 2960 bs, 1680 s, 1600 s, 1439 s, 1351 m, 1316 m, 1142 s, 1100 m, 1052 m, 992 s, 770 bs, 669 m, 525 vs. ¹H NMR: δ 8.44 (dxd, 2 H, J₁ = 5.3, J₂ = 1.3), 7.73 (txd, 2 H, J₁ = 7.7, J₂ = 2), 7.42 (d, 2 H, J = 8.1), 7.15 (m, 2 H), 6.20 (dxd, 1 H, J₁ = 9, J₂ = 3, H₃), 6.12 (dxd, 1 H, J₁ = 9, J₂ = 3, H₂), 3.28 (m, 1 H, H₅), 2.88 (broad, 1 H_{7a}), 2.80 (broad, 1 H, H_{7b}), 1.54 (m, 2 H, H_{1,4}), 1.27 (dxd, 1 H, J₁ = 8.3, J₂ = 2.1, H_{5a}), 1.05 (d, (broad), J₁ = 8.3, H_{5b}); ¹³C NMR δ 149.0, 137.9, 137.2 (C₂), 132.6 (C₃), 122.6, 121.8, 50.0 (C₇), 45.96 (C₄), 44.4 (C₁), 42.7 (C₅), 30.6 (C₆). Elemental analysis calcd. for C₁₈H₁₇N₃O (M_w = 291.35): C 74.20, H 5.88, N 14.42; found C 74.38, H 6.01, N 14.39.

X-ray Measurement and Structure Determination of I. A single crystal was mounted on a glass fiber in inert oil and transferred to the cold gas stream of a Siemens P4 four circle diffractometer equipped with a LT-2 low-temperature unit. The unit cell parameters were determined and refined from 26 randomly selected reflections in the range of 5.4 to 11.0, obtained by P4 automatic routines. Data were measured via ω-scans and corrected for Lorentz and polarization effects, but not for absorption. The structure was solved by direct methods

(SHELXS-86)⁴⁹ and refined by full-matrix least-squares against F².⁵⁰ The function minimized was [w(F_o² – F_c²)]² with the weight defined as w⁻¹ = 2(F_o²) + (xP)² + yP and P = (F_o² + 2F_c²)/3. All non-hydrogen atoms were refined with anisotropic displacement parameters. All hydrogen atoms were located by difference Fourier methods, but in the refinement they were generated geometrically and refined with isotropic displacement parameters 1.2 times higher than U(eq) of the attached C atoms. The norbornenyl group is disordered (1:1) in two orientations and has overlying atoms C(2), C(3), C(5), and C(7), which were refined with the same parameters (position and displacement) for each of the both directions. C(3), C(5), and C(7) were shared in C(3a) = C(7b), C(5a) = C(5b), and C(7a) = C(3b) for the calculation of the hydrogen atoms. Further crystallographic data are collected in Table 1.

Reaction with Pd²⁺. PdCl₂ (0.356 g, 2.0 mmol) was added to a stirred solution of **I** (0.373 g, 1.28 mmol) in 20 mL of methanol at 60 °C. The mixture was stirred for 14 h and the resulting precipitate was collected by filtration in quantitative yield. It was washed extensively with methanol and dried in vacuo. Elemental analysis calcd for C₁₈H₁₇Cl₂N₃OPd (M_w = 468.678 gmol⁻¹): C 46.13, H 3.66, N 8.97, found C 46.01, H 3.38, N 8.98. MS (ESI⁺, DMF/methanol): calcd for C₃₆H₃₄N₆O₂Pd₂Cl₃: 898.988; found: 898.77.

Investigation of the Living Character of the Polymerization. Five test tubes, each containing a stirred solution of the monomer (100 mg, 0.34 mmol) in methylene chloride (10 mL) were placed in a Schlenk tube. Indicated amounts of initiator, dissolved in methylene chloride were added to the stirred solutions of the monomer. All solutions were stirred for 2 h, ferrocene carboxaldehyde (10-fold excess based on initiator) was added, and stirring was continued for 1 h. Finally, all solutions were poured on pentane (50 mL). Polymers obtained as white solids were filtered off and dried in vacuo. Except for the highly soluble 10- and 15-mers, which were obtained in 50 and 60% yield, respectively, yields were quantitative.

Poly(N,N-bipyridyl-endo-norborn-2-ene-5-carbamide)₁₀: M_w calcd 3240, found (vs polystyrene) 3300 gmol⁻¹, PDI = 1.80; IR (KBr, cm⁻¹) 2940 m, 1676 s, 1585 s, 1570 s, 1465 s, 1433 s, 1381 m, 1250 bs, 779 s, 746 s, 698 m (cis =CH δ oop). ¹H NMR δ 8.39 (m, broad, 2 H), 7.71 (m, broad, 2 H, 2), 7.34 (m, broad, 2 H), 7.15 (m, broad, 2 H), 5.5 (dxd, broad, 2 H, H_{2,3}), 4.35 (m) 4.06 (m), 4.02 s (Cp), 3.16 (m, broad, 1 H), 2.6 (m, broad, 2 H), 1.93 (dxd, broad, 2 H), 1.38 (m, broad, 2 H); ¹³C NMR δ 175 (C₁₃), 154.8 (C₈), 148.9 (C₁₀), 138.0 (C₁₂), 134.1, 130.3, 127.9, 125.2, 122.6 (C₁₁), 121.9 (C₉), 69.2 (Cp), 47.6 (C₅), 41.6 (C₁), 40.8 (C₄), 40.0 (C₇), 37.6 (C₆).

Preparation of the Cross-Linked Polymers. The following procedure is typical. **III** (0.53 g, 0.75 mmol) was added to a stirred solution (300 rpm) of **I** (5.7 g, 19.6 mmol) in 300 mL of methylene chloride. After 50 min, **II** (11.4 mL, 10.86 g, 68.7 mmol) was added to the solution and stirring was continued for 10 h. Finally, benzaldehyde (1 mL) was added in order to ensure quantitative termination of reaction. After 1 h, the polymer was filtered off, washed with methylene chloride, and dried in vacuo. The crude product was cleaned by stirring in hydrochloric acid (400 mL, 1 M) for 72 h, followed by aqueous ammonia (200 mL, 10%) for 10 h. Washing with methanol and diethyl ether yielded 17.86 g (97.1%) of an off-white powder.

Acknowledgment. The authors thank Univ.-Doz. Dr. K.-H. Ongania for carrying out the ESI-MS measurements as well as Univ.-Doz. Dr. P. Peringer for the recording of the NMR data. Special thanks to G. Seeber for the interpretation of the GPC-derived data. Financial support was provided by the Austrian National Science Foundation (FWF, Vienna, Austria), project number P-11740-GEN, and the European Commission, project number F14 W-CT96-0019. M. Mupa thanks the Austrian Academic Exchange Service (ÖAD) for a doctoral fellowship, project number 897/97.

JA973495+

(49) Sheldrick, G. M. *SHELXS-86: Program for Crystal Structure Solutions*; University of Göttingen: Göttingen, 1986.

(50) Sheldrick, G. M. *SHELXL-93: Program for the Refinement of Crystal Structures*; University of Göttingen, Göttingen, 1993.